

SOME ASPECTS OF THE FINE STRUCTURE IN A TURBULENT BOUNDARY LAYER

S. RAJAGOPALAN# AND R.A. ANTONIA

DEPARTMENT OF MECHANICAL ENGINEERING

UNIVERSITY OF NEWCASTLE, NSW. 2308 AUSTRALIA

#PRESENT ADDRESS: DEPARTMENT OF MECHANICAL ENGINEERING, UNIVERSITY OF ADELAIDE, S.A. 5000 AUSTRALIA

SUMMARY Digital data acquisition and processing has been used to generate the envelope of band-pass filtered velocity and temperature fluctuations measured at different Reynolds numbers. Using a method similar to that of Rao et al (1971) for detecting the fine structure, the frequency f_p of this structure is found to scale on outer variables for part of the layer which excludes the near-wall region. Smoothing of the envelope results in good agreement between the magnitude of f_p and that obtained by earlier investigators using a visual discriminating procedure. Conditional averages associated with the fine structure suggest the presence of vortex-like structures in the boundary layer.

INTRODUCTION

It has been established that both the large structure and the fine structure of a turbulent boundary layer have identifiable properties. It has also been suggested that a dynamic interaction exists between the outer flow and the bursting phenomenon which occurs near the wall. Kim et al's (1971) flow visualisation study showed that the frequency of bursting f_b scales on outer flow variables, namely the free stream velocity U_1 and the boundary layer thickness δ . Rao et al (1971) identified high frequency pulses in the longitudinal velocity fluctuation u in a boundary layer with bursting. They found, over a region of the layer extending down to the sublayer, that the frequency f_p of high frequency pulses also scales on U_1 and δ . Recent experiments have indicated conflicting trends with regard to the scaling of f_b . Alfredsson and Johansson (1982) found that in the near-wall region of a duct neither inner nor outer variables were appropriate scales for f_b . They also report comments by Blackwelder and Haritonidis who challenge Rao et al's (1971) claim for outer scaling in the near-wall region on the grounds that Rao et al's measurements may have been affected by inadequate spatial resolution of their hot wire. Blackwelder and Haritonidis' conclusion that f_b , measured in a boundary layer, scales on inner variables has not been supported by the boundary layer measurements of Andreopoulos et al (1983).

Leaving aside the apparently unresolved question of what is the appropriate scaling for the frequency of bursting, the scaling of f_p on U_1 and δ points to the possibility of a special relationship or interaction between the large structure and the fine structure.

The properties of the large structure in a slightly heated turbulent boundary layer have been studied by Chen and Blackwelder (1978) using a rake of cold wires. They observed that a sharp gradient in temperature fluctuation θ associated with the upstream boundary of outer layer bulges extended to the wall region. Chen and Blackwelder suggested that the zone of rapid change in θ , as well as u and the velocity fluctuation v normal to the wall, could be identified with an internal front which may provide the dynamic link between the outer flow and the bursting phenomenon. From space-time correlations of wall shear stress and velocity fluctuations, Thomas and Brown (1977) interpreted bursting as the response of the wall region to the passage of the large structure. The interaction between the large and the fine structures has been studied by Brown and Thomas (1977) in a boundary layer and Rajagopalan and Antonia (1980) in a fully developed duct flow using space-time correlations of low and high frequency components of velocity and wall shear stress fluctuations.

In addition to the previous interaction studies, proper-

ties of the large structure such as its frequency of occurrence and conditional averages associated with it have been considered by Chen and Blackwelder (1978) and Antonia et al (1982). Conditional averages of the fine structure have not been reported.

In the present work the fine structure is identified using a method similar to that introduced by Rao et al (1971) and adopted by others (e.g. Antonia et al, 1976; Badri Narayanan et al, 1977). While a visual discrimination procedure was used by Rao et al (1971) to identify the fine structure, the present approach uses digital data acquisition and processing in an effort to minimise the unavoidable subjectivity associated with visual discrimination. The fine structure has been identified using either velocity or temperature fluctuations. Conditional averages associated with the fine structure have been obtained and compared with averages associated with the large structure.

The smallest value of y/δ considered in this study is 0.045. This corresponds to a value of about 44 for yU_τ/ν (U_τ is the friction velocity, ν is the kinematic viscosity of the fluid) at a Reynolds number $R_m (= U_1 \delta_2/\nu, \delta_2$ is the momentum thickness) of about 3000, the minimum Reynolds number before the velocity and temperature fields can be assumed to be approximately Reynolds number independent (e.g. Antonia et al, 1982). The present study does not therefore provide information on the fine structure in the near-wall region.

EXPERIMENTAL SETUP

The boundary layer developed on the smooth floor of a low speed wind tunnel with a $0.3 \text{ m} \times 0.25 \text{ m}$ working section. The first 3 m of the floor was heated to provide a constant wall heat flux distribution. The boundary layer was tripped near the beginning of the test section using a 3 mm dia. rod. Simultaneous measurements of u , v and θ were made using a X-wire/cold wire arrangement. The hot wires (1 mm long) were made of $5 \mu\text{m}$ Pt-10% Rh wire and operated with two DISA 55M10 anemometers and DISA 55M25 linearisers. The cold wire, mounted 1.2 mm upstream of the centre of the X-wire, was made of $0.6 \mu\text{m}$ Pt-10% Rh wire and was operated by a constant current (0.1 mA) circuit. The hot and cold wires were calibrated in the potential core of a heated jet. Signals from the hot wires were corrected for temperature contamination.

Signals from the X-wire/cold wire arrangement were recorded on a Hewlett-Packard 3968A FM tape recorder at a speed of 38.1 cm/sec. Two Krohn-Hite filters (3323) and a DISA 55M26 signal conditioner, operated in the band-pass mode, with a variable bandwidth Δf and centre frequency f_c , were used to obtain band-pass filtered signals u , v and θ . Signals proportional to u , v and θ

and band-pass filtered u , v and θ were digitised using a 12 bit A/D converter at a sampling frequency of $2.5f_c$ and stored and processed on a PDP 11/34 computer. Measurements were made in nearly self-preserving conditions at $x = 2.3$ m for six values of R_m . A summary of experimental conditions covering the present range of R_m is given in Antonia et al (1982, Table I).

FORMATION OF CONDITIONAL AVERAGES OF THE FINE STRUCTURE

The generation of the envelope of high frequency pulses, which is the basis for the fine structure identification, was carried out on the computer. Successive local maxima were first identified in the digital band-pass filtered signals and a linear interpolation scheme was subsequently used to interpolate between the maxima. The pulse frequency f_p is determined by counting the number of times the envelope exceeds a particular threshold level. Envelopes corresponding to positive ($\equiv p$), negative ($\equiv n$) and absolute ($\equiv a$) parts of high frequency pulses associated with a fluctuation β ($\equiv u, v$ or θ) are denoted by $H_\alpha(\beta)$ where $\alpha \equiv p, n$ or a . Traces of u , band-pass filtered u and $H_p(u)$ are shown in Figure 1. Small amplitude, small scale fluctuations in the envelope (arrows in Figure 1) made a significant contribution to f_p . This contribution can be minimised by smoothing the envelope $H_\alpha(\beta)$. Note that the generation of the envelope already entails some smoothing. In this work, the smoothing of $H_\alpha(\beta)$ was achieved by forming the envelope, denoted as $\hat{H}_\alpha(\beta)$ of $H_\alpha(\beta)$. Figure 1 shows that small scale fluctuations in $H_p(u)$ are nearly eliminated in $\hat{H}_p(u)$.

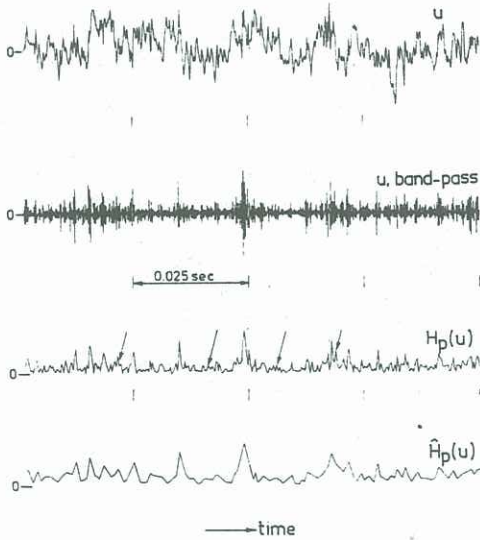


Figure 1 Traces of the longitudinal velocity fluctuation u , band-pass filtered u , envelope $H_p(u)$ of the positive part of the band-pass filtered u and smoothed envelope $\hat{H}_p(u)$. $R_m = 4750$, $y/\delta = 0.43$.

To calculate conditional averages associated with the fine structure, the instants of time denoted by τ_n ($n = 1, \dots, N$ where N is the total number of detections) when this structure is detected, are determined when $H_\alpha(\beta)$ or $\hat{H}_\alpha(\beta)$ reaches a maximum immediately following the condition

$$H_\alpha(\beta) \text{ or } \hat{H}_\alpha(\beta) > k \beta' \quad (1)$$

Here k is the threshold level and a prime indicates an rms value. Conditional averages are then obtained as

$$\langle \beta(t) \rangle = \frac{1}{N} \sum_{n=1}^N \beta(\tau_n + t) \quad (2)$$

The instants τ_n are arbitrarily aligned at $t = 0$ in the

averaging process. N was set equal to 300.

AVERAGE FREQUENCY OF PULSES

The average frequencies f_p and \hat{f}_p were determined for envelope signals H and \hat{H} respectively, and the mean periods between pulses are denoted by \bar{T} ($\equiv f_p^{-1}$) and $\bar{\hat{T}}$ ($\equiv \hat{f}_p^{-1}$). It was observed that the variation of f_p with k was independent of bandwidth in the range $0.05 < \Delta f/f_c < 0.3$ at $R_m = 4750$ and $y/\delta = 0.43$. Results presented here were obtained with the upper and lower cut-off frequencies of the band-pass filter set equal to f_c , thus providing the minimum bandwidth. It was observed that changing $\Delta f/f_c$ in the range 0.05 to 0.3 did not alter the location, in time, of the maxima in the envelopes. Distributions of the normalised average frequency f_p^* ($\equiv f_p \delta / U_1$, an asterisk denoting normalisation by U_1 and δ), estimated from $H_\alpha(\beta)$ are shown in Figure 2 at $R_m = 4750$ and $y/\delta = 0.045$. The dependence of f_p on k is similar to that already reported by Rao et al (1971) and Badri Narayanan et al (1977). The maximum value f_{pm} in the

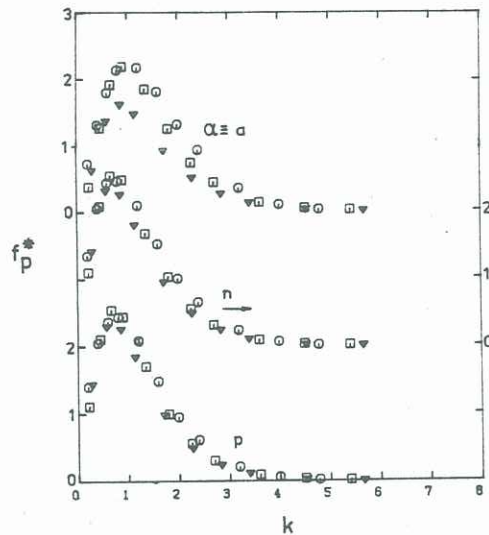


Figure 2 Normalised frequency of occurrence of pulses estimated using $\hat{H}_\alpha(\beta)$. $R_m = 4750$, $y/\delta = 0.43$. \square , $\beta = u$; \circ , v ; ∇ , θ .

variation of f_p with k has been identified with the frequency of bursting by Rao et al and with the frequency of the fine structure by Badri Narayanan et al. Rao et al obtained a constant value of 2.5 for \bar{T}_b^* ($\equiv \bar{T}_b f_b^*$) across the boundary layer. In the present work, the normalised mean period \bar{T}_m^* , where $\bar{T}_m = f_{pm}^{-1}$, is approximately 0.4, irrespective of whether α is positive or negative and whether u or v was used in forming $H_\alpha(\beta)$. Estimates of f_{pm} using θ were smaller by 10-20% than those obtained using u or v . Estimates of the pulse frequency \hat{f}_p , obtained using \hat{H} , were expectedly smaller than f_p , since the contribution due to small scale fluctuations is reduced when \hat{H} is used instead of H . The magnitude of \hat{f}_{pm} was consistently smaller than f_{pm} and was independent of whether \hat{H}_p or \hat{H}_n was used. The period \bar{T}_m^* was approximately 1.7 at $R_m = 4750$ and $y/\delta = 0.43$, close to the value of 1.5 of Badri Narayanan et al and Ramaprian and Shivaprasad (1982) who used a visual discrimination procedure to obtain f_p . Antonia et al (1976) obtained a value of 0.5 for \bar{T}_m^* and suggested that a visual discrimination procedure is likely to favour large amplitude excursions of high frequency pulses and therefore yield a smaller pulse frequency. The present observation that the removal of small scale fluctuations in H decreases the pulse frequency supports this suggestion.

Figure 3 indicates that \bar{T}_m^* is approximately constant

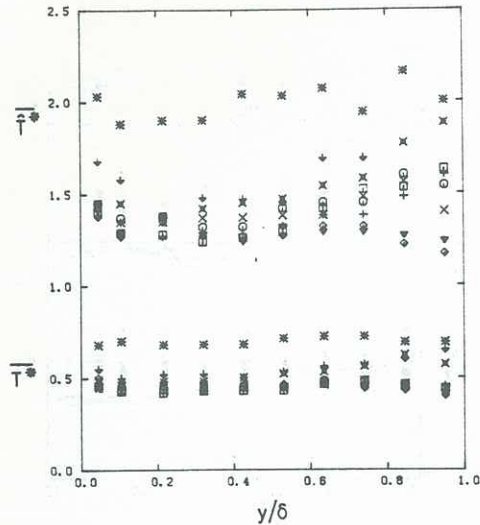


Figure 3 Variation across the boundary layer of the average period associated with the fine structure. $R_m = 4750$. \bar{T}^* and \bar{T}_m^* are inferred from $H_{\alpha}(\beta)$ and $\hat{H}_{\alpha}(\beta)$ respectively. $\alpha = p$: \square , $\beta = u$; $+$, v ; \diamond , θ . $\alpha = n$: \circ , u ; \times , v ; \sqcup , θ . $\alpha = a$: ∇ , u ; \diamond , v ; $*$, θ .

over the present range of y/δ whereas \bar{T}_m^* is approximately constant only in the region $0.1 < y/\delta < 0.7$. The present values of \bar{T}_m^* are in good agreement with those of Antonia et al (1976) whereas the \bar{T}_m^* distribution is in close agreement with that of Badri Narayanan et al (1977) and Ramaprian and Shivaprasad (1982). Figure 4 indicates that \bar{T}_m^* or \bar{T}^* is approximately independent of R_m when $R_m \geq 2000$.

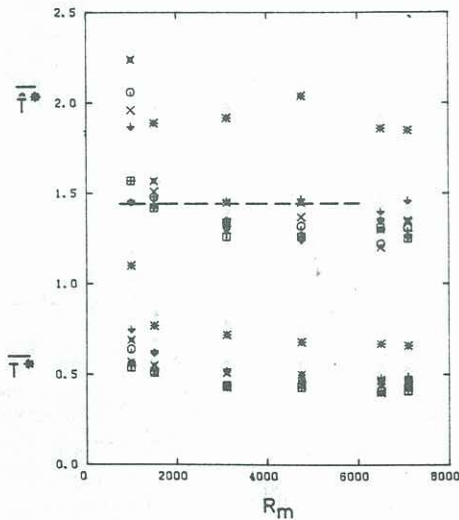


Figure 4 Reynolds number dependence of average period associated with the fine structure at $y/\delta \approx 0.4$. Symbols as for Figure 3. —, Badri Narayanan et al (1977).

CONDITIONAL AVERAGES

Conditional averages associated with the fine structure were obtained for a value of k which yielded $f_p^* \approx 0.4$, the value corresponding to the average frequency of the temperature fronts. This latter frequency was deter-

mined by Subramanian et al (1982) on the basis of visual identification of these fronts using a rake of cold wires and was deemed to be more reliable than estimates obtained using one-point conditional techniques. The present choice of k was made to minimise any ambiguity which may arise when comparing fine structure averages with large structure averages. Typical results at $R_m = 4750$ and $y/\delta = 0.045$ are shown in Figure 5.

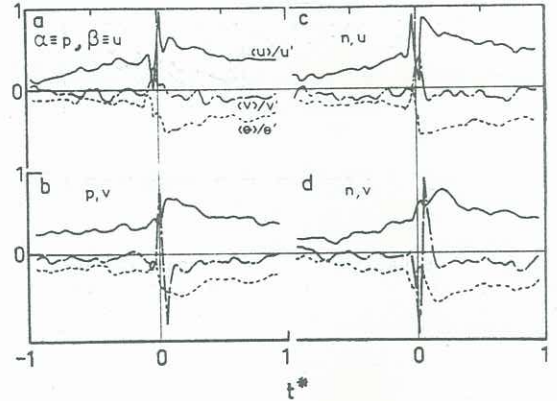


Figure 5 [a] Conditional averages from $H_p(u)$; [b] Conditional averages from $H_p(v)$; [c] Conditional averages from $H_n(u)$; [d] Conditional averages from $H_n(v)$.

The distribution of $\langle u \rangle$ based on $H_p(u)$ [Figure 5a] increases gradually until $t^* = -0.1$. Near $t^* = 0$, $\langle u \rangle$ first decreases rapidly to zero, followed by a rapid increase before a subsequent slow decrease. In contrast, $\langle v \rangle$ is approximately zero and $\langle \theta \rangle$ is negative everywhere. Averages $\langle u \rangle$ and $\langle \theta \rangle$, based on $H_p(v)$ [Figure 5b] are positive and negative respectively. They increase and decrease respectively near $t^* = 0$. The distribution of $\langle v \rangle$ is reminiscent of the velocity distribution associated with a vortex structure. Averages based on $H_p(\theta)$ did not show any characteristic shape near $t^* = 0$. The distribution of $\langle u \rangle$ based on $H_n(u)$ has a different shape near $t^* = 0$ (Figure 5c) compared to the distribution based on $H_p(u)$; the distribution of $\langle v \rangle$ based on $H_n(v)$ is almost the mirror image of that (Figure 5b) based on $H_p(v)$.

It is of interest to compare conditional averages associated with the fine structure with those for the large structure. In Figure 6, fine structure averages based on $H_p(\theta)$ are compared with the large structure averages obtained using VITA applied to θ . Although there is general qualitative agreement, differences can be observed. For example, the magnitude of changes near $t^* = 0$ is larger in the VITA average than in the fine structure average. Whereas the distribution of $\langle u \rangle$ based on $H_p(\theta)$ is always positive, the VITA distribution for $\langle u \rangle$ changes sign near $t^* = 0$. Similarly, the distribution of $\langle \theta \rangle$ based on $H_p(\theta)$ is essentially negative whereas the VITA distribution for $\langle \theta \rangle$ changes sign near $t^* = 0$. In Figure 7, averages based on $H_a(\theta)$ are compared with those obtained using a technique similar to that of Brown and Thomas (1977) in which the temperature fluctuation is first high-pass filtered and subsequently rectified and smoothed. The averages were then obtained using Eqs. (1) and (2) after replacing β with θ and H_{α} by the rectified and smoothed high-pass filtered signal. The comparison (Figure 7) is favourable except for a small phase shift which is probably caused by the effective hold time in smoothing the rectified, high-pass filtered signal.

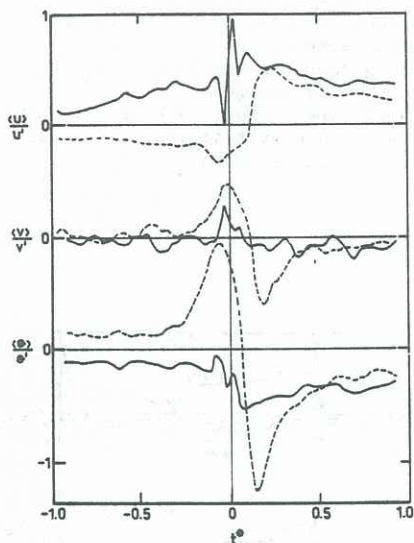


Figure 6 Comparison of conditional averages of the fine structure with those of the large structure, obtained using VITA. —, fine structure; ---, large structure.

CONCLUSIONS

The scaling of the average pulse frequency on outer variables supports the conclusion of previous investigations in which visual discrimination was used for the identification of the fine structure. Quantitative agreement between these investigations and the present approach, for the pulse frequency, is achieved only after smoothing is applied to the envelope in the present work. Conditional distributions of u and v , based on the positive and negative parts of the envelope exhibit characteristic changes near the instant of detection and suggest the presence of small scale, vortex-like structures with clockwise and counter-clockwise components.

ACKNOWLEDGEMENT

The support of the Australian Research Grants Scheme is gratefully acknowledged.

REFERENCES

- ALFREDSSON, P. H. and JOHANSSON, A. V. (1982) Time-scales for Turbulent Channel Flow, Report TRITA-MEK-82-11 R. Inst. Techn., Stockholm.
- ANDREOPOULOS, J., DURST, F., JOVANOVIĆ, J. and ZARIC, Z. (1983) Influence of Reynolds Number on Characteristics of Turbulent Wall Boundary Layers, submitted to *J. Fluid Mech.*
- ANTONIA, R. A., DANH, H. Q. and PRABHU, A. (1976) Bursts in Turbulent Shear Flows, *Phys. Fluids*, **19**, 1680-1686.
- ANTONIA, R. A., RAJAGOPALAN, S., SUBRAMANIAN, C. S. and CHAMBERS, A. J. (1982) Reynolds Number Dependence of the Structure of a Turbulent Boundary Layer, *J. Fluid Mech.*, **121**, 123-140.

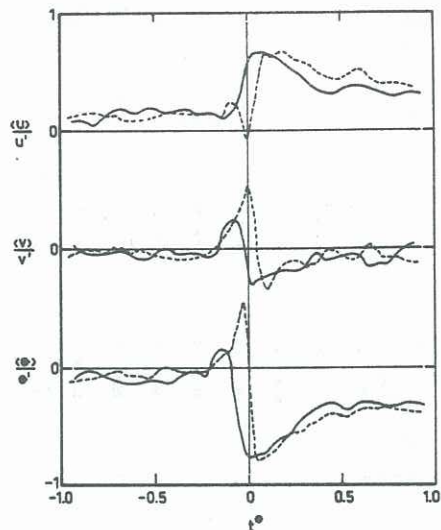


Figure 7 Comparison of conditional averages of the fine structure (solid curves) with those obtained (broken curves) using a method similar to that of Brown and Thomas (1977) and Thomas and Brown (1977).

BADRI NARAYANAN, M. A., RAJAGOPALAN, S. and NARASIMHA, R. (1977) Experiments on the Fine Structure of Turbulence, *J. Fluid Mech.*, **80**, 237-257.

BROWN, G. L. and THOMAS, A. S. W. (1977) Large Structure in a Turbulent Boundary Layer, *Phys. Fluids*, **20**, S243-S252.

CHEN, C-H. P. and BLACKWELDER, R. F. (1978) Large Scale Motion in a Turbulent Boundary Layer: A Study Using Temperature Contamination, *J. Fluid Mech.*, **89**, 1-31.

KIM, H. T., KLINE, S. J. and REYNOLDS, W. C. (1971) The Production of Turbulence Near a Smooth Wall in a Turbulent Boundary Layer, *J. Fluid Mech.*, **50**, 133-160.

RAJAGOPALAN, S. and ANTONIA, R. A. (1980) Interaction Between Large and Small Scale Motions in a Two-Dimensional Turbulent Duct Flow, *Phys. Fluids*, **23**, 1101-1110.

RAMAPRIAN, B. R. and SHIVAPRASAD, B. G. (1982) The Instantaneous Structure of Mildly Curved Turbulent Boundary Layers, *J. Fluid Mech.*, **115**, 39-58.

RAO, K. N., NARASIMHA, R. and BADRI NARAYANAN, M. A. (1971) The Bursting Phenomenon in a Turbulent Boundary Layer, *J. Fluid Mech.*, **48**, 339-352.

SUBRAMANIAN, C. S., RAJAGOPALAN, S., ANTONIA, R. A. and CHAMBERS, A. J. (1982) Comparison of Conditional Sampling and Averaging Techniques in a Turbulent Boundary Layer, *J. Fluid Mech.*, **123**, 335-362.

THOMAS, A. S. W. and BROWN, G. L. (1977) Large Structure in a Turbulent Boundary Layer, *Proc. Sixth Australasian Hydraulics & Fluid Mechanics Conference*, 407-410.